ON CLOUD STRUCTURE NEARBY ABLATING HYDROGEN PELLETS

B.V. Kuteev and A.Yu. Kostrukov

State Technical University, 195251, St.Petersburg, Russia

1. Introduction

A cigar shape of the luminous clouds which surround hydrogen pellets ablating in high temperature plasmas has been observed in many tokamak and stellarator experiments [1]. Although understanding of the mechanisms responsible for the cloud shape formation would be very helpful for further development of ablation models and analysis of cloud instabilities, there are problems with theoretical description of experimental data available.

The estimations of the cloud transverse size on the basis of numerical hydrodynamic codes (see [2] and references inside) give a reasonable agreement with experiment at high plasma parameters but do not allow to evaluate the longitudinal size of the cloud and significantly overestimate the transverse size at the plasma periphery.

In this paper we consider a quasi-stationary solution for the luminous cloud region. Analyzing experimental data on pellet cloud luminosity we try to define main processes responsible for the luminous cloud shape. The results of simple estimations of the luminous region parameters are compared with numerous high speed photos from T-10 [3] and an integrated photo from Tore Supra [4].

2. Experimental cloud structure

A typical luminosity distribution in a cloud [3] is shown in Fig. 1. The film exposure time was 5 μs. The photo shows a back view for a pellet moving towards the plasma center from the low field side. The contour lines correspond to constant luminosity levels in a logarithmic scale. The following features
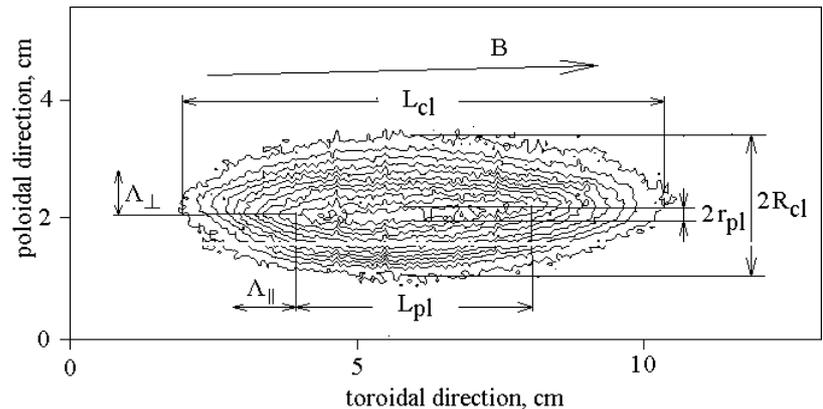

Fig. 1. Luminous cloud contour plot.

of the cloud should be emphasized. The cloud has a cigar shape plateau with approximately constant level of the luminosity (inside the most internal contour). The plateau radius r_{pl} is approximately constant along all the cloud and is usually 2-3 times larger than the pellet radius r_p, while the plateau length L_{pl} is much larger than r_p. The plateau seems to be straight. Outside the plateau the luminosity decays exponentially with a characteristic length Λ. The

decay length along the magnetic field $\Lambda_{\parallel}$ is a bit greater than the decay length across the magnetic field $\Lambda_{\perp}$. The temperature along the cloud plateau is weakly varied nearby 1-2 eV as well as the gas density [5-7].

A schematic cloud structure corresponding to the features mentioned above is shown in Fig. 2. Usually only the total cloud sizes R_{cl} and L_{cl} are considered, which values depend on the detection limit of framing cameras.
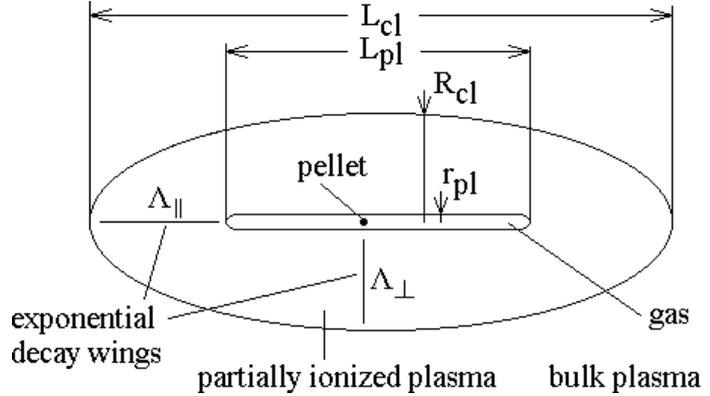

Fig. 2. Schematic cloud structure.

3. Luminous plateau radius

When the cloud moving across the magnetic field becomes partially ionized the friction force arises between ions and neutrals. This force stops the transverse motion of the gas flow. The effective radius where the ionization begins provided by the hydrodynamic codes [8, 2] is $(2-3)r_p$. To avoid complicate calculations we estimate r_{pl} from the power which is necessary for ionization of all ablated atoms [9]

$$E_{loss}\, dN/dt = 2\pi r_{pl}^2 \frac{1}{4} n_e \sqrt{\frac{8T_e}{\pi m_e}} 2T_e \tag{1}$$

Here E_{loss}=1+1+2+13.6 eV, the energy spent for heating, acceleration, dissociation and ionization of the neutrals, m_e is the electron mass, dN/dt is the Parks scaling ablation rate [10].

Another estimation for the r_{pl} can be made using the spherical neutral gas shielding model [11] and Saha ionization degree. The model predictions for the neutral cloud temperature T_{cl}, the total density N_{cl} and the electron density N_e are shown in Fig. 3. (H$_2$-pellet, r_p=0.05 cm, T_e=500 eV, n_e=3.5×10^{-13}cm^{-3}, dN/dt=1.7×10^{23} atom/s). The maximal electron density is N_{cl} = 7×10^{17} cm^{-3} and the cloud temperature in the point of maximal density T_{cl} = 1-2 eV.
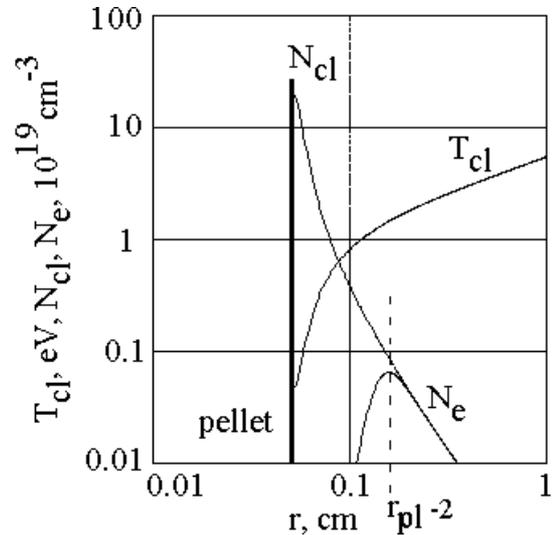

Fig. 3. Cloud parameters calculated within the spherical NGS model [11].

Fig. 4 shows plateau radii for different stages of the pellet ablation in T-10 (#49968). r_{pl}-1 is obtained from the Eq. (1) and r_{pl}-2 is modeled by Saha ionization. Both approaches used yield r_{pl} values which agree well with the experimental ones. At the plasma border the

Saha approach overestimates the plateau radius likely due to neglected ionization caused by the bulk plasma electrons. In the minor radius interval 12 cm $< r <$ 16 cm striated clouds were observed. This explains deviation of the points in this interval from the general dependence.

4. Longitudinal plateau size

The experiments show that the cloud has constant parameters several centimeters along the plateau. This allows us to conclude that the gas is confined in the longitudinal direction. The spherical approach predicts the cloud pressure at the ionization radius $N_{cl}T_{cl}$ significantly greater than the external plasma pressure $n_iT_i+n_eT_e$. Actually, ionization of the gas near r_{pl} modifies the spherical gas cloud expansion into a one dimensional extension inside a "plasma tube". The gas extends along the magnetic field providing the constant

Fig. 4. Plateau radii and ablation rate.

pressure. The particle flow $\Gamma \equiv dN/dt$ through the gas cloud surface must not change compared with the spherical case. Particle velocity v_{cl} corresponds to the sound velocity at 1eV temperature and is approximately constant. While the cloud surface enlarges, N_{cl} obtained from the spherical model reduces by the same factor. The expression for the length to radius ratio L_{pl}/r_{pl} can be then written down as follows

$$2\pi r_{pl}L_{pl}v_{cl}\left(n_eT_e + n_iT_i\right) = 4\pi r_{pl}^2 v_{cl}N_{cl}T_{cl}, \quad N_{cl} = \frac{dN/dt}{4\pi r_{pl}^2 v_{cl}} \Rightarrow L_{pl} = \frac{\left(\dfrac{dN/dt}{2\pi r_{pl}v_{cl}}\right)T_{cl}}{n_eT_e + n_iT_i} \tag{2}$$

Fig. 5 shows L_{pl} calculated from Exp. (2) for T-10 (#49968). Good agreement with the experimental plateau length L_{pl} seems to be surprising after a number of simplifications made. The same comparison for Tore Supra [4] with the pellet/plasma parameters substantially different from T-10 also provided reasonable values for L_{pl} (see Fig. 6).

5. The luminous cloud wings

For description of the transverse and longitud-inal decay lengths of clouds a model developed

Fig. 5. Plateau lengths

for the divertor plasma [12] can be applied. Similarly to divertor plasmas the main effect responsible for the distribution of neutrals and ions is a diffusion like process governed by
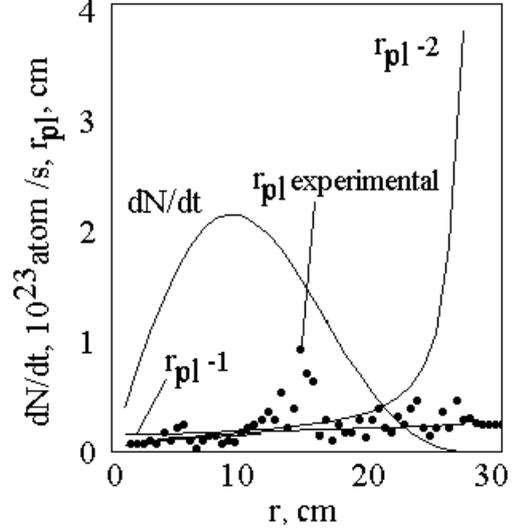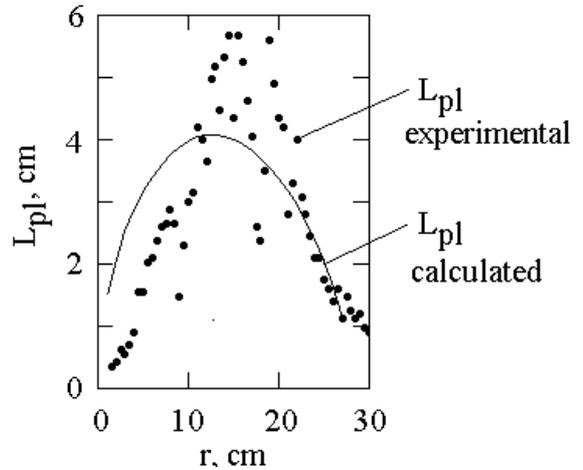
simultaneous charge exchange and ionization of neutrals. For this case the distribution of neutrals penetrating into the bulk plasma is an exponential function with the characteristic decay length

$$\Lambda \sim \left(\frac{\lambda_{ex}\lambda_{ion}}{3} \right)^{\frac{1}{2}} \qquad (3)$$

Here $\lambda_{ion} = v_{cl}/N_{cl}<\sigma v>_{ion}$ is the length of ionization due to secondary plasma electrons, v_{cl} is the gas thermal velocity, $\lambda_{ex} \approx 1/\sigma_{ex}N_{cl}$ is the characteristic length for charge exchange in the secondary plasma. With the temperature $T_{cl} = 1.5$ eV, Eq. (3) yields a good prediction for evolution of the decay length while the pellet penetrates into the plasma.

Fig. 6. Tore Supra track photo [4] and simulation.

6. Summary

The clouds look like a luminous plateau surrounded by exponential wings. The plateau corresponds to a quasi-stationary gas region. Across the magnetic field the gas is confined in a "tube" by the partially ionized plasma. The longitudinal expansion of the gas cigar maintains the gas pressure equal to the bulk plasma pressure. The exponential decay wings observed are explained by a diffusion like motion of neutrals into the bulk plasma. The plateau and wings' parameters agree with those obtained in T-10 and Tore Supra experiments.

Acknowledgments

References

[1] Milora, S.L., Houlberg, W.A., Lengyel, L.L., Mertens, V., Nucl. Fusion, **35** 657 (1995).
[2] Kristof, G., Lengyel, L., Europhys. Conf. Abstracts, **21A,** P.IV, 1553 (1997).
[3] Egorov, S.M., Kuteev, B.V., Miroshnikov, I.V., et al. Nucl. Fusion, **32** 2025 (1992).
[4] Pegourie, J.-M., Picchiottino, H.-W., Drawin, A., et. al. Nucl. Fusion, **33** 591 (1993).
[5] Sergeev, V.Yu., Kostrukov, A.Yu., Shibaev, S.A., Fus. Eng. and Design, **35** 323 (1997).
[6] Durst, R.D., Rowan, W.L., Austin, R.A., et al., Nucl. Fusion, **30** 3 (1990).
[7] McNeill, D.H., Greene, G.J., Schuresco, D.D., Phys. Rev. Lett., **55** 1398 (1985).
[8] Kaufmann, M., Lackner,K., Lengyel,L., and Schneider, Nucl. Fusion, **26** 171 (1986).
[9] Houlberg, W.A., Milora, S.E., Attenberger, S.E., Nucl. Fusion, **28** 595 (1988).
[10] Parks, P.B., Turnbull, R.J., Phys. Fluids, **21** 1945 (1978).
[11] Kuteev, B.V., et al. Fusion Technology, **26** 642 (1994).
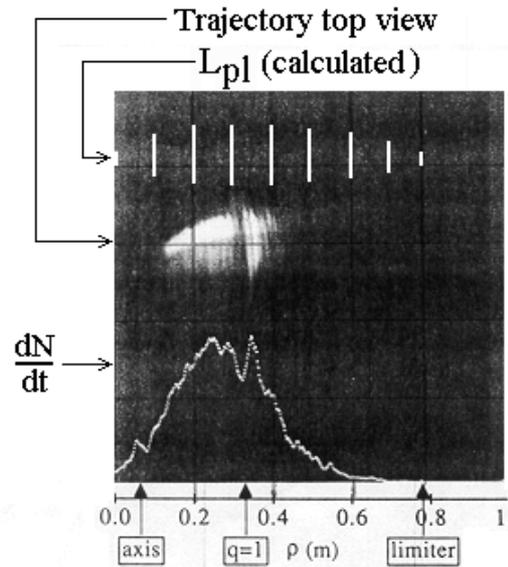[12] Krasheninnikov S.I. et al., Phys. Plasmas, **2** 2717 (1995).